Interaction of pyridine with acidic (H-ZSM5, H-beta, H-MORD zeolites) and superacidic (H-Nafion membrane) systems: An IR investigation

ARTICLE *in* LANGMUIR · FEBRUARY 1996

Impact Factor: 4.46 · DOI: 10.1021/la950571i

5 AUTHORS, INCLUDING:

Gabriele Ricchiardi
Università degli Studi di Torino
89 PUBLICATIONS **4,314** CITATIONS
SEE PROFILE

Carlo Lamberti
Università degli Studi di Torino
379 PUBLICATIONS **13,123** CITATIONS
SEE PROFILE

A. Zecchina
Università degli Studi di Torino
560 PUBLICATIONS **19,933** CITATIONS
SEE PROFILE

Interaction of Pyridine with Acidic (H-ZSM5, H-β, H-MORD Zeolites) and Superacidic (H-Nafion Membrane) Systems: An IR Investigation

R. Buzzoni, S. Bordiga,* G. Ricchiardi, C. Lamberti,† and A. Zecchina

Dipartimento di Chimica Fisica Chimica Inorganica e Chimica dei Materiali dell'Università di Torino, Via P. Giuria 7, I-10125 Torino, Italy

G. Bellussi

ENI RICERCHE, Via F. Maritano 26, I-20097 S. Donato (Mi), Italy

Received July 10, 1995. In Final Form: October 23, 1995[⊗]

The interaction of pyridine with acidic H-ZSM5, H-β, and H-MORD zeolites and a perfluorosulfonic superacidic membrane (H-Nafion) has allowed us to study the IR spectrum of PyH^+ hydrogen bonded to the negative zeolite skeleton (Z^-) or to $CF_2SO_3^-$ groups of the membrane. In the presence of excess Py the formation of $PyH^+\cdots Py$ is also detected. On H-MORD (a zeolite with higher Al content) the adsorption of Py at room temperature is limited to the external surfaces of the crystallite, owing to the blockage of channel mouths caused by the PyH^+ formed in high concentration. The IR spectra of hydrogen-bonded PyH^+ in the $\nu(NH\cdots)$ stretching region are strongly influenced by Fermi resonance effects with the overtones and combinations of low-frequency modes. In the H-Nafion/Py system the modification induced by the proton transfer on the internal modes of the $-SO_3H$ groups (with formation of SO_3^- species) gives additional information on the proton transfer process. To complete the assignment of all the observed surface species (including the weakly adsorbed ones) the interaction of Py with silicalite (a purely siliceous zeolite with a pentasilic structure) has also been investigated.

1. Introduction

Protonic zeolites, sulfated zirconia, and heteropolyacids on one side and sulfonated polymers on the other side are important acidic and superacidic catalysts in several reactions involving carbocationic intermediates.[1−4] To fully understand the role of acidity in the catalytic processes, it is vital to know the elementary steps of the interaction of various molecules with the acidic groups and the possible role of hydrogen-bonded precursors. This problem is particularly important when the interaction of H_2O, CH_3OH, and $O(CH_3)_2$ (molecules playing a role in many catalytic reactions) with H-ZSM-5, H-β, H-MORD, and H-Y is considered. The structure of the possible interaction products is usually investigated by means of vibrational techniques, among which IR spectroscopy is emerging as the most informative. However it is not always possible from IR spectra to unambiguously distinguish hydrogen bonded and protonated species. This fact is related to the high complexity of the IR spectra of strongly hydrogen-bonded species because the shape of the bands (very broad) is usually complicated by Fermi resonance effects with the overtones of the low-frequency modes.[5−8] The solution of this complicated problem could receive decisive help from the systematic study of the IR spectra of the interaction products of a complete series of bases characterized by proton affinities in a wide range and a series of solids with acidic and superacidic character.

Following this idea, in this investigation we present and discuss the spectra of the interaction products of a strong base (Py) of high proton affinity with four different solids with strongly acidic (H-ZSM-5, H-β, and H-MORD) and superacidic (H-Nafion) character. The resulting spectra are then compared with those of Py adsorbed on a similar MFI porous structure (silicalite) not containing Brönsted acidity. A similar approach can be easily found in the literature[9−13] (see, for example, the work of Borade et al. and references therein) where, however, a comparison with undoubtedly superacidic systems is absent. This investigation is part of a complete series of studies concerning the interaction of the same acids with bases of smaller proton affinities like CH_3CN, CH_3OH, $O(CH_3)_2$, and H_2O. The study of the interaction products with the opposite end members (*i.e.*, very weak bases like CO or N_2) has already been initiated and partially published.[14−16]

2. Experimental Section

IR spectra of zeolites were taken of samples in the form of thin self-supporting pellets. Silicalite, H-ZSM-5 (Si/Al = 15) and H-MORD (Si/Al = 5) have been synthesized and kindly supplied by ENICHEM laboratories in Novara (Italy), while H-β (Si/Al = 12.5) has been prepared in the laboratories of ENI RICHERCHE

* Author to whom correspondence should be addressed.
† Also with INFN Sezione di Torino.
⊗ Abstract published in *Advance ACS Abstracts,* January 15, 1996.

(1) Yamaguchi, T. *Appl. Catal.* **1990**, *61*, 1.
(2) Misono, M.; Okuhara, T. *Chemtech* **1993**, ***Nov.***, ***23***.
(3) Arata, K. *Adv. Catal.* **1990**, *37*, 165.
(4) Hölderich, W.; Hesse, M.; Näumann, F. *Angew. Chem., Int. Ed. Engl.* **1988**, *27*, 226.
(5) Evans, J. C. *Spectrochim. Acta* **1960**, *16*, 994.
(6) Claydon, M. F.; Sheppard, N. *Chem. Commun.* **1969**, 1431.
(7) Bratos, S. *J. Chem. Phys.* **1975**, *63*, 3499.
(8) Bratos, S.; Ratajczak, H. *J. Chem. Phys.* **1982**, *76*, 77.
(9) Borade, R. B.; Adnot, A.; Kaliagnuine, S. *J. Chem. Soc., Faraday Trans.* **1990**, *86*, 3949.
(10) Ghosh, A. K.; Curhoys, G. *J. Chem. Soc., Faraday Trans.* **1983**, *79*, 805.
(11) Borade, R. B.; Clearfield, A. *J. Chem. Soc., Faraday Trans.* **1995**, *9*, 539.
(12) Parker, L. M.; Bibby, D. M.; Burns, G. R. *J. Chem. Soc., Faraday Trans.* **1991**, *97*, 3319.
(13) Emeis, C. A. *J. Catal.* **1995**, *141*, 347.
(14) Zecchina, A.; Bordiga, S.; Spoto, G.; Scarano, D.; Petrini, G.; Leofanti, G.; Padovan, M.; Otero Areán, C. *J. Chem. Soc., Faraday Trans.* **1992**, *88*, 2959.
(15) Bordiga, S.; Lamberti, C.; Geobaldo, F.; Zecchina, A.; Turnes Palomino, G.; Otero Areán, C. *Langmuir* **1995**, *11*, 527.
(16) Geobaldo, F.; Lamberti, C.; Ricchiardi, G.; Bordiga, S.; Zecchina, A.; Turnes Palomino, G.; Otero Areán, C. *J. Phys. Chem.* **1995**, *99*, 11167.

0743-7463/96/2412-0930$12.00/0

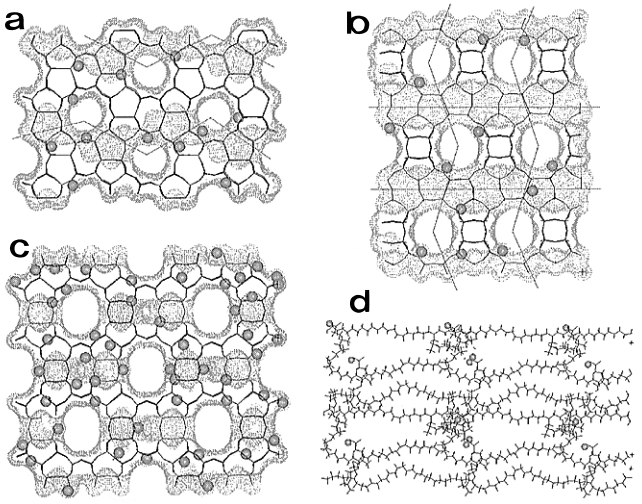

Figure 1. The tridimensional structure of the H-zeolites and of H-Nafion: (a) H-ZSM-5, (b) H-β, (c) H-MORD, and (d) H-Nafion. The pore volumes are evidenced by dotted surfaces, and the channels running perpendicular to the observation direction are evidenced by lines. The positions of protons (randomly distributed) are represented by spheres.

in San Donato (Mi, Italy). In the case of Nafion polymer a thin self-supporting film, obtained from a solution of Nafion in a aliphatic/alcohol/water mixture (purchased from Aldrich), has been prepared.

The FTIR spectrometer was a Bruker 66 instrument and the spectral resolution 4 cm^{-1}. Computer graphic and molecular mechanics simulations have been performed with programs by Biosym Technologies,[17] running on a SGI workstation.

3. The Structure of Silicalite, H-ZSM-5, H-β, H-MORD, and H-Nafion: General Considerations

The reactivity of Py with these systems is largely determined by the nature of the porosity of the materials and by their acid site concentrations, which determine the diffusion rates and adsorbed amounts. For this reason a brief description of the structures will precede the experimental results section.

In Figure 1 the structures of the materials under study are shown using the following conventions: (i) the structural frameworks are shown with sticks, including all atoms; (ii) acidic sites are shown as spheres on the H positions, randomly distributed over the allowed positions according to the aluminum contents; (iii) zeolite porosity is described by the solvent accessible surface calculated according to the Connolly algorithm.[18] The dotted surface decribes the boundary between the accessible and non-accessible regions of the lattice: channels parallel to the observation direction appear as circular white regions while those perpendicular to it appear as bands of dots and are highlighted with lines.

3.1. Silicalite and H-ZSM-5 (Figure 1a) have the same MFI framework structure and differ in chemical composition: silicalite is a silica polymorph while H-ZSM-5 is an aluminosilicate with H^+ as counterion (Si/Al ratio = 15 in our sample). The MFI structure forms a three-dimensional network of channels defined by 10-membered rings. One family of straight channels runs in the [010] direction (the observation direction in Figure 1a), and a second family of sinusoidal channels runs in the [100] direction and connects the straight ones. The location of counterions is not accessible to experimental observation (especially in dehydrated samples[19] but simulations[20] suggest that preferred positions are on low-angle Si−O−A1 bridges pointing toward the cavities. The size of the channels is enough to allow Py diffusion through all parts of the structure and allows it to interact with all acid sites.[20] The three-dimensional nature of the channel system and the low density of H^+ counterions prevent its occlusion by adsorbed molecules.

3.2. Zeolite H-β (Figure 1b) is another high-silica aluminosilicate (Si/Al = 12.5 in our sample) characterized by two sets of perpendicular straight channels defined by 12-membered rings and running in the [100] and [010] directions. The intersections of these main channels produce a third set of curved channels running in the [001] direction whose geometry depends on the stacking sequence.[21] Channel intersections define cavities allowing freedom of movement to more than one Py molecule. As in the case of H-ZSM-5 the cavity system cannot be easily occluded by adsorbed molecules. Also for H-β zeolite hydrogen positions are unknown and the aluminum distribution is thought to be random.[22]

3.3. Mordenite (Figure 1c) is a zeolite with higher Al content (Si/Al ratio = 5) which has a set of parallel straight channels running along the [001] direction, defined by 12-membered silicate rings. The channels have side pockets in the [010] directions which are too small for Py penetration. The higher Al content implies a higher concentration of acid sites, which we assume to be randomly distributed over channels and pockets. This fact, together with the unidirectional nature of the channel system, causes the diffusion of Py to be hindered by adsorbed molecules. Moreover, acid sites in the side pockets are not accessible to Py.

3.4. H-Nafion (Figure 1d) is a perfluorosulfonic polymer

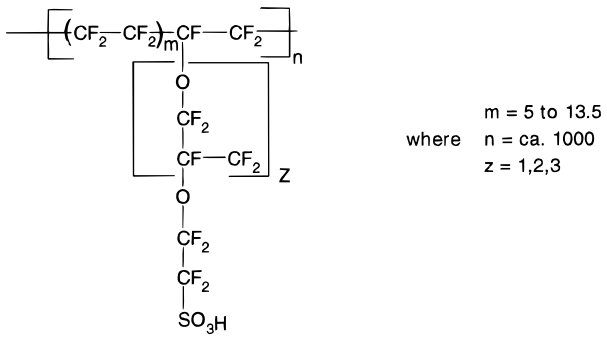

where the fluorine atoms confer on the SO_3H groups an extremely high acidity. The three-dimensional structure of the disordered compound is not known. Our attempts to build realistic models of the polymer with a combination of molecular graphics, molecular mechanics, and ab-initio calculations are reported elsewhere.[23,24]

For the scope of the interpretation of the experiments reported here, we will assume a model consisting of fibers of parallel disordered chains. Sulfonic groups on the

(17) InsightII and Discover User Guide, Biosym Technology, San Diego, California, 1993.
(18) Connolly, M. L. *Science* **1983**, *221*, 709.
(19) Mortier, W. J. *Compilation of extraframework sites in zeolites*, Butterworth: Leuven, Belgium, 1982.
(20) Redondo, A.; Hay, P. J. *J. Phys. Chem.* **1993**, *97*, 11754.
(21) Higgins, J. B.; La Pierre, R. B.; Schlenker, J. L.; Rohrman, A. C.; Wood, J. D.; Kerr, G. T.; Rohrbaugh, W. J. *Zeolites* **1988**, 48, 446.
(22) Pápai, I.; Goursot, A.; Fajula, F.; Weber, J. *J. Phys. Chem.* **1994**, *98*, 4654.
(23) Ricchiardi, G.; Ugliengo, P. 1st Electronic Computational Chemistry Conference, Department of Chemistry, Northern Illinois University of Kalb, IL, Nov 7−18, 1994; Poster 69.
(24) Buzzoni, R.; Bordiga, S.; Ricchiardi, G.; Spoto, G.; Zecchina, A. *J. Phys. Chem.* **1995**, *99*, 11937.

lateral chains can interact by strong hydrogen bond forming regions with polar character.

The access to acid sites is regulated by the polymer flexibility: in dehydrated samples the polymer is highly packed while the diffusion of Py involves its swelling to form an open structure.

4. The Adsorption and Desorption Experiments at Room Temperature: A Preliminary Discussion on the Selected Experimental Conditions and the Experimental Results

Py is a very basic and strongly interacting molecule. Hence, when it impinges on the external surfaces of the zeolite crystallites it is immediately strongly adsorbed with formation of an external layer, while the inner surfaces remain unaffected. In the external layer all acidic groups have reacted with the Py molecules (saturation and supersaturation region); while in the bulk the acidic centers are unreacted. After this quick initial step, Py starts to diffuse in the bulk through the channel system. In the presence of diffusion limitations, two regions are present which are separated by a narrow front which is moving gradually toward the interior of the particles with the amount of the dosed Py. This is the reason why during the adsorption experiments at room temperature (RT) (*vide infra*) only the spectra of fully saturated and supersaturated layers (H^+/Py ratios ≤ 1) are constantly obtained (although with an intensity increasing with dosage). In the case of H-MORD the initial doses of Py (from the gas phase) cause the blockage of the channel entrances and prevent the further movement of the penetration front toward the interior of the crystals: in this case the total adsorbed amount is very small because it is limited to the external layer and at the channel entrances. The reasons for the different behavior of H-ZSM-5 and H-β on one side and H-MORD on the other side will be discussed in the following: for the time being we only anticipate that it is mainly associated with the different size of the channels and the different concentration of H^+ sites. In conclusion, as diffusion problems represent a severe difficulty in RT experiments and because adsorption and desorption temperatures higher than 300 K must be avoided (because of the extreme reactivity of the acidic systems under investigation) the presented spectra are usually reported during Py desorption. Adsorption experiments of Py on the pure siliceous material (silicalite) have also been realized to obtain reference spectra of physisorbed Py (*vide infra*).

The same considerations also substantially hold for the interaction of Py with H-Nafion. In this case, besides the effects already mentioned for the zeolites (associated with the high enthalpy of the acid−base interaction) leading to the immediate formation of an external layer of strongly adsorbed Py, we must consider that diffusion of Py toward the internal part of the fibrous polymer can occur only if it is accompanied by a complex rearrangement of the polymeric chain conformation (swelling) which is indeed a slow, diffusion-controlled, process. From this point of view the basic differences between the four systems can be summarized as follows: (i) for H-ZSM-5 and H-β, the penetration front moves quickly toward the interior taking also advantage of their intersecting channel systems which facilitate the diffusion inside the crystallites; (ii) for H-MORD, the penetration front is blocked on the external layers; (iii) for H-Nafion, the H^+Py interaction initially occurs at the external surface; however, (unlike mordenite) the penetration front is not blocked because of the fluxional character of the polymer and so it can slowly proceed toward the interior of the polymer particles up to the complete consumption of the acidic groups.

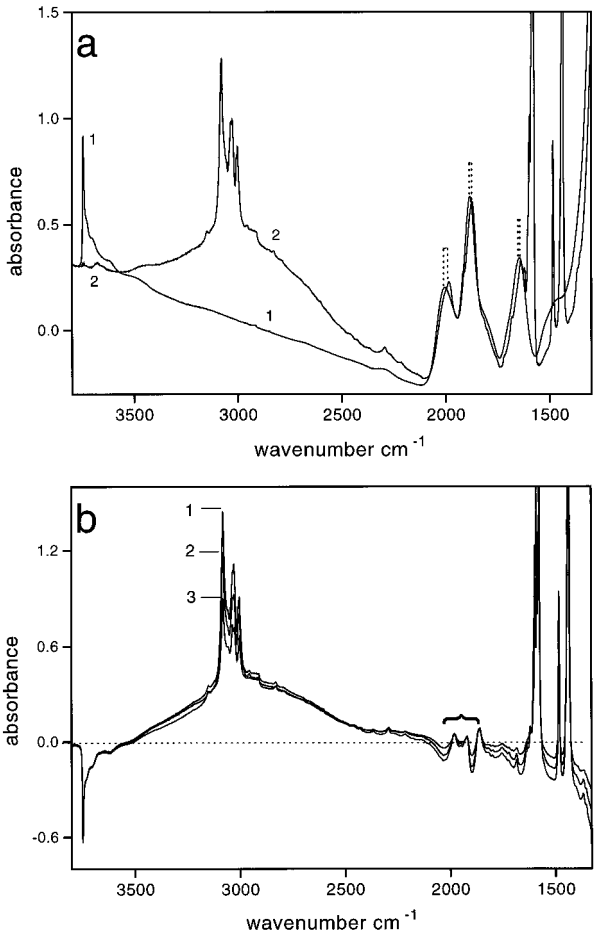

Figure 2. (a) Curve 1: silicalite background spectrum after outgassing under vacuum at 973 K. Curve 2: spectrum after equilibration with vapor pressure of Py; the shifts of the overtone and combination modes in the 2000−1600 cm^{-1} range caused by Py adsorption are evidenced. (b) Curve 1: background-subtracted spectrum of silicalite equilibrated with vapor pressure of Py. Curves 2 and 3: silicalite sample with increasing outgassing time at room temperature. The braces indicates the position of the most prominent oscillations due to small shifts occurring in the overtone and combination modes upon Py adsorption.

On the basis of these preliminary considerations the experimental conditions were selected as described below:

4.1. Silicalite. The samples, preliminarily outgassed under vacuum at 973 K to remove adsorbed H_2O (spectrum 1, Figure 2a), were contacted with the vapor pressure of Py at RT (spectrum 2, Figure 2a) and then outgassed for increasing times at RT to gradually remove the adsorbed Py (Figure 2b, curves 1−3: the spectra are background subtracted). In this type of representation the bands appearing with negative values correspond to consumed species while the positive bands correspond to newly formed species. The spectral regions concerning Py bands have been also reported in Figure 3.

The scope of the experiment was the determination of the IR spectra of Py hydrogen bonded to silanols and of Py simply physically adsorbed in the channels (and not interacting with any specific site).

4.2. H-ZSM-5. The spectrum of the sample outgassed at 673 K, in the 3800−3600 cm^{-1} region is characterized not only by the presence of the bands at 3750 cm^{-1} (attributed to silanols), and at 3609 cm^{-1} (assigned to Brönsted sites) but also by a non-negligible absorption at 3670 cm^{-1}. This ν(OH) band has already been discussed in ref 14; bands at similar frequencies have also been

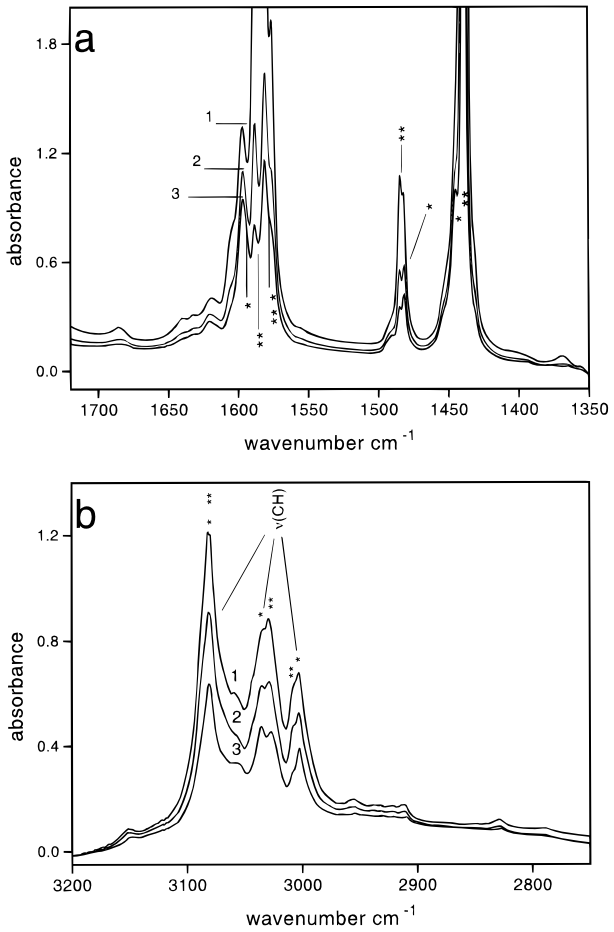

Figure 3. (a) Curves 1−3: enlargements of the corresponding spectra of Figure 2b. One asterisk indicates H-bonded (hb) Py; two asterisks indicate physisorbed (ph) Py. (b) Curves 1−3: details of Figure 2b; one asterisk indicates (hb) Py; two asterisks indicate (ph) Py.

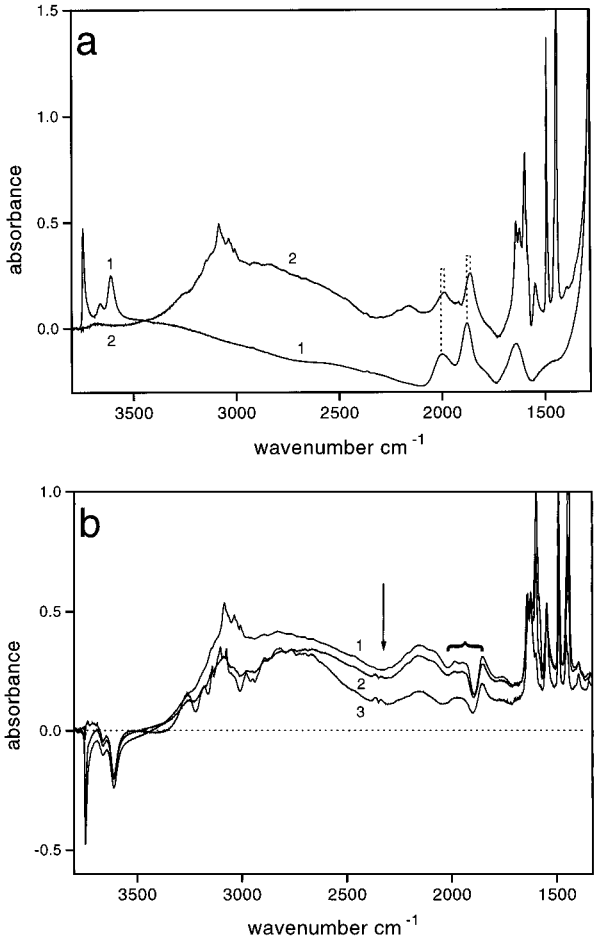

Figure 4. (a) Curve 1: H-ZSM-5 background spectrum after outgassing under vacuum at 673 K. Curve 2: spectrum after equilibration with vapor pressure of Py. (b) Curve 1: background-subtracted spectrum of H-ZSM-5 equilibrated with vapor pressure of Py. Curves 2 and 3: spectra at increasing outgassing time at room temperature. Oscillations in the overtone and combination mode region (due to small shifts upon Py adsorption) are indicated with braces. The arrow indicates an Evans window caused by Fermi resonance of the ν(NH···) with 2 × γ(NH$^+$···N) mode of the (PyH$^+$···P) dimer.

found in other zeolite systems.[25−28] They have been ascribed to hydroxyl groups attached to extraframework aluminum. When probed with CO at 77 K and with other molecules, the acidity of these species seems lower than that of bridged Brönsted sites but higher than that of any other OH groups of γ-alumina.[14] For this reason the band at 3670 cm^{-1} has been assigned to OH groups in partially extralattice positions with intermediate acidic character.

The samples, previously outgassed at 673 K under vacuum, have been contacted with Py vapor at the saturation pressure to completely fill the pores (H-ZSM-5, Figure 4a, spectrum 2, and Figure 4b, spectrum 1; under these conditions the H$^+$/Py ratio is ≤1). Notice that spectra 1−3 of Figure 4b are background subtracted. The H$^+$/Py ratio is then gradually increased by outgassing for increasing times at RT to remove the weakest interacting species; after prolonged pumping the spectrum does not change further (spectrum 3 of Figure 4b). This spectrum corresponds to strongly adsorbed PyH$^+$ species (H$^+$/Py ∼ 1) in the channels and cavities of H-ZSM-5. Independent gravimetric measurements confirm that, after prolonged outgassing at ∼340 K (estimated sample temperature under the IR beam), the H$^+$/Py ratio is approaching 1. No efforts have been made to extend the gravimetric measurements to higher Py equilibrium pressures. To better illustrate the complexity of the situations, expanded portions of the spectra are illustrated in Figure 5 (particularly spectrum 3 in Figure 4b).

4.3. H-*β*. The samples outgassed at 673 K have been successively contacted with increasing Py dosages to obtain complete pore filling. In the case of β zeolite Py diffusion is faster than in ZSM-5 zeolite. Since equilibrium is attained at each Py dosage, spectra could be recorded directly during adsorption. The zeolite background and the spectrum obtained under saturation conditions are illustrated in Figure 6a (spectra 1 and 2, respectively) to allow a complete comparison with the data reported on H-ZSM-5. The spectra obtained with increasing coverages of Py are reported in Figure 6b (curves 1−3, background subtracted). As far as the quantitative estimation of the H$^+$/Py ratio after prolonged outgassing, at ∼340 K under the IR beam, is concerned, the same procedure adopted for H-ZSM-5 has been used. Also in this case the region of Py and Py$^+$ modes is reported in a separate figure (Figure 7a). The spectrum reported in Figure 7b is a blowup of curve 1 in Figure 6b.

4.4. H-MORD. The procedure followed for H-MORD is identical to that adopted for H-ZSM-5. The results are shown in Figure 8 and 9. Although the internal volume

(25) Sayed, M. B.; Kidd, R. A.; Cooney, R. P. *J. Catal.* **1984**, *88*, 137.
(26) Kustov, L. M.; Kazansky, V. B.; Beran, S.; Kubelkovà, L.; Jirù, P. *J. Phys. Chem.* **1987**, *91*, 5247.
(27) Loeffler, G. L.; Lohse, U.; Peuker, Ch.; Oehlmann, G.; Kustov, L. M.; Zholobenko, V. L.; Kazansky, V. B. *Zeolites* **1990**, *10*, 266.
(28) Fritz, P. O.; Lunsford, J. H. *J. Catal.* **1989**, *118*, 85.

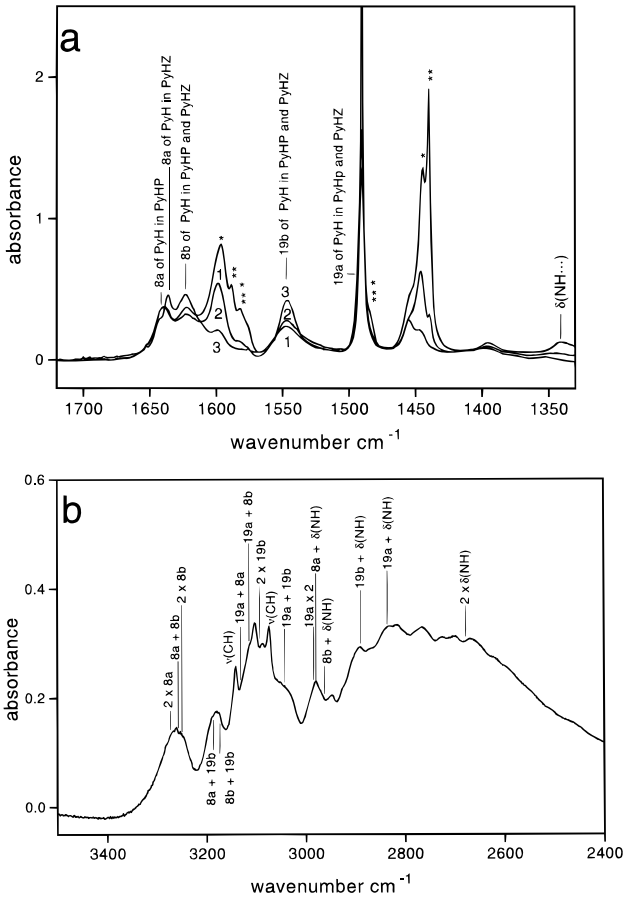

Figure 5. (a) Curves 1−3: enlargements of the corresponding spectra of Figure 4b. One asterisk indicates (hb) Py; two asterisks indicate (ph) Py; PyH indicates pyridinium species; PyHP indicates pyridinium H-bonded with pyridine; and PyHZ indicates pyridinium H-bonded with the negatively charged zeolitic framework (Z^- in the text). (b) Details of spectrum 3 of Figure 4b. The calculated overtone and combinations of the bands shown in Figure 5a are indicated by lines. The assignment is done without considering the selection rules.

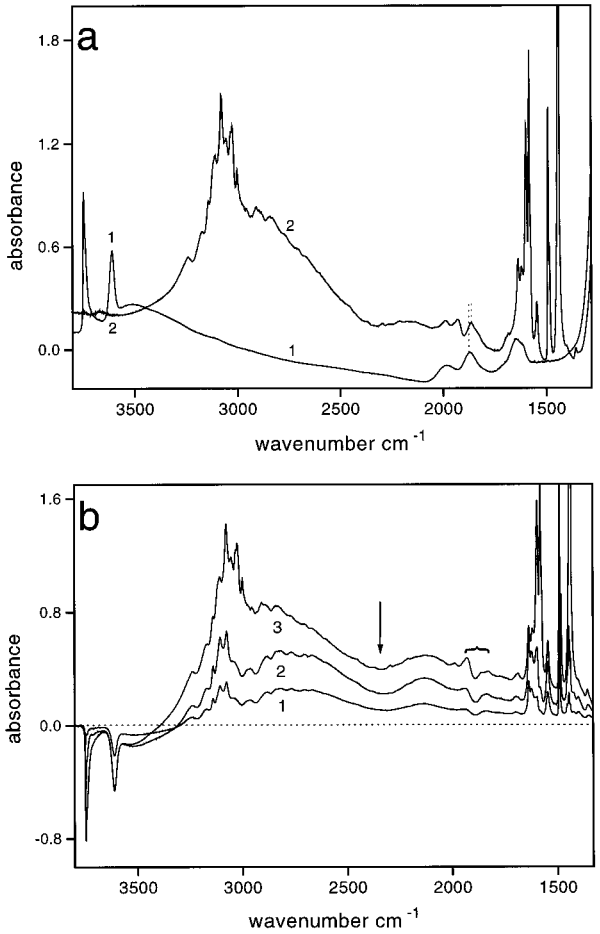

Figure 6. (a) Curve 1: H-β background spectrum after outgassing under vacuum conditions at 673 K. Curve 2: spectrum after equilibration with vapor pressure of Py. (b) Curves 1 and 2: background-subtracted spectra of H-β at increasing Py dosages. Curve 3: spectrum of H-β equilibrated with vapor pressure of Py. Braces and arrow indicate analogous features to those in Figure 4b.

and the main channel radii of H-MORD and H-ZSM-5 are similar, H-MORD Brönsted sites are only partially eroded upon Py dosages and the intensity of the bands due to adsorbed Py is definitely at least 1 order of magnitude smaller than on H-ZSM-5. As the same difference was not observed for weaker bases like N_2,[16] CO[14,15] C_2H_4,[29] etc., it is inferred that Py is adsorbed only on the external surfaces and at the channel mouth. To verify if a different adsorption procedure could modify this unexpected result, we have carried out adsorption experiments from the pure Py liquid phase (instead of from the gas phase) following an *in situ* procedure (also prolonging the contact time to $^1/_2$ h). The results were practically identical, and they are not described here for the sake of brevity. From this we have concluded that the small Py adsorption has not a kinetic character (as it should have if diffusion is mainly responsible) and that mouth occlusion is the most plausible mechanism explaining the small Py uptake.

4.5. H-Nafion. The procedure adopted for H-Nafion follows the same lines described before for the other systems. In the present case, however, the equilibration with saturated Py vapor takes more time to be completed, because of the diffusion limitations associated with the swelling process of the membrane. The results are shown in Figure 10 and 11. Unlike the previous cases, the frequency region below 1000 cm^{-1} can be investigated in detail (because the skeletal modes of the polymeric chains do not obscure all the other manifestations). For more details see ref 24.

5. The IR Spectra of Py Species on Silicalite (Figures 2 and 3): Hydrogen-Bonded and Physically Adsorbed Py

Upon Py adsorption all silanol groups are consumed (disappearance of the tailed band with a maximum at 3745 cm^{-1}) with formation of a strong and broad absorption (fwhm, ≈550 cm^{-1}) centered at about 3000 cm^{-1} ($\Delta\nu \cong 700$ cm^{-1}): this is due to the reaction

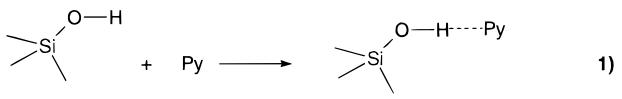

1)

which leads to the formation of 1:1 silanol−Py adducts. It is more interesting to notice also the presence of a broad satellite band at ≈2300 cm^{-1} likely associated with a Fermi resonance with the overtone of the δ(OH) mode of the silanol groups involved in hydrogen bonding with Py (which is consequently localized at ≈1150 cm^{-1}) as found for the silica/Py system.[30] An interesting effect to be noticed is the small shift induced by the Py adsorption on

(29) Spoto, G.; Bordiga, S.; Ricchiardi, G.; Scarano, D.; Zecchina, A.; Borello, E. *J. Chem. Soc., Faraday Trans.* **1994**, *90*, 2827.

(30) Parry, E. P. *J. Catal.* **1963**, *2*, 371.

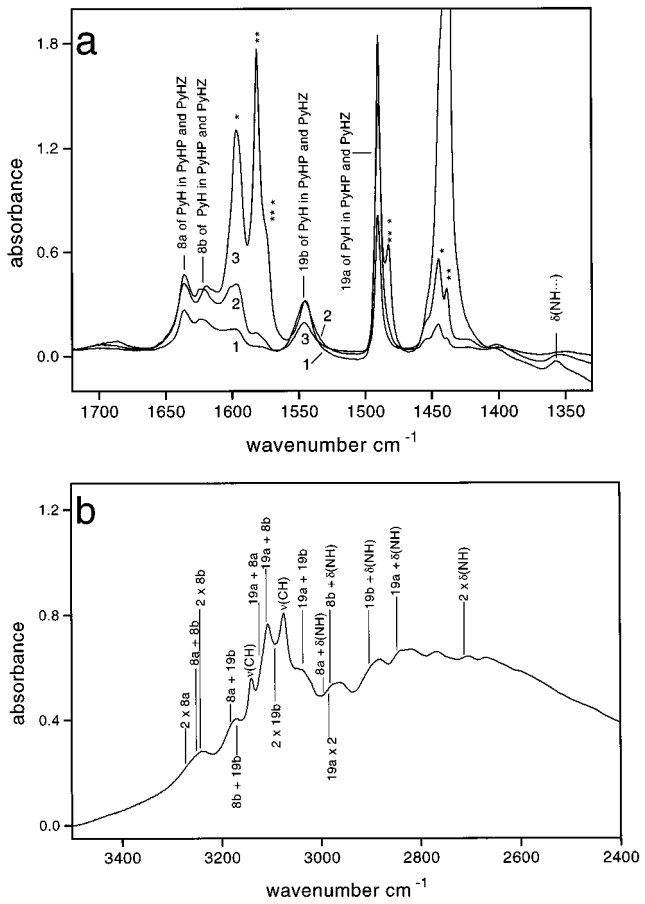

Figure 7. (a) Curves 1−3: details of the corresponding spectra of Figure 6b. One asterisk indicates (hb) Py; two asterisks indicate (ph) Py; PyH indicates pyridinium species; PyHP indicates pyridinium H-bonded with pyridine; and PyHZ indicates pyridinium H-bonded with the negatively charged zeolite framework. (b) Details of spectrum 1 of Figure 6b. The overtones and combinations of the bands shown in Figure 7a are indicated by lines. The assignment is done without considering the selection rules.

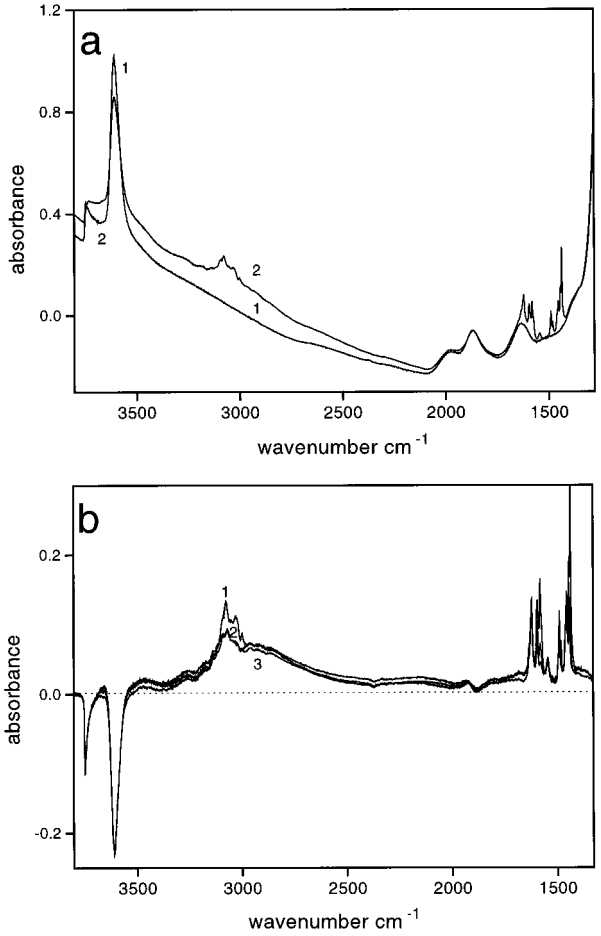

Figure 8. (a) Curve 1: H-MORD background spectrum after outgassing under vacuum conditions at 673 K. Curve 2: spectrum after equilibration with vapor pressure of Py. (b) Curve 1: background-subtracted spectrum of H-MORD equilibrated with vapor pressure of Py. Curves 2 and 3: spectra at increasing outgassing times at room temperature.

the skeletal combination modes observed at 2005, 1884, and 1645 cm^{-1} *in vacuo* and at 1986, 1872, and 1637 cm^{-1} after Py adsorption (as indicated in Figure 2a). Similar effects are also present for the other combination modes at ≅1450 cm^{-1}: however, they will not be considered in detail because they are less clearly observed. In the difference spectra these small shifts appear as oscillations (see braces in Figure 2b). These bands must not be confused with the modes of the adsorbed species, as they are only indicating that the filling of the pores with Py slightly modifies the frequencies of the skeletal modes. This effect is largely unspecific and will also be observed practically unmodified on the other zeolites.

The ring stretching modes of hydrogen-bonded (hb) and physically (ph) adsorbed Py are clearly observed at 1597 (hb, mode 8a), 1588 (ph, mode 8a), 1581 (hb, ph, mode 8b), 1485 (ph, mode 19a), 1481 (hb, mode 19a), 1444 (hb, mode 19b), and 1439 cm^{-1} (ph, mode 19b). These two types of species, when characterized by different frequencies, can be easily distinguished on the basis of their different behavior upon desorption at RT, as the hydrogen-bonded species is the most strongly adsorbed. The modes with prevailing ν(CH) stretching character are in the 3100−3000 cm^{-1} range (bands at 3081, 3036−3028, and 3007−3002 cm^{-1}).[31] In the figures hb and ph are indicated with one and with two asterisks, respectively.

(31) Kline, C. H.; Turkevich, J. *J. Chem. Phys.* **1944**, *12*, 300.

The spectroscopic properties of the silanol−Py complexes can so be schematically shown as follows:

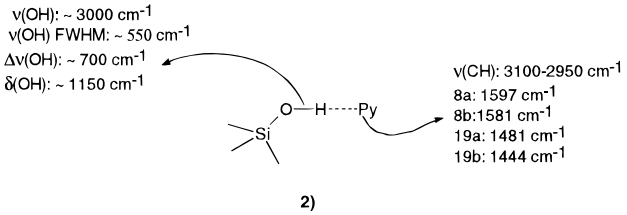

2)

As a final observation let us draw attention to the small bands in the 2960−2900 cm^{-1} interval (Figure 3b) which we attribute to overtones and combinations of the Py ring stretching modes in the 1480−1425 cm^{-1} range. Also the other ring modes in the 1600−1570 cm^{-1} interval (8a, 8b, and 19b) can (in principle) give overtones in the 3200−3100 cm^{-1} interval:[31] for instance the weak peak at 3150 cm^{-1} seems to be easily assigned to the overtone of the 1581 cm^{-1} fundamental. These overtones (usually less prominent in liquid Py) have likely gained some intensity because of a moderate enhancement effect due to Fermi resonance with the broad band centered at ≈3000 cm^{-1} due to the ν(OH···Py) mode of hydrogen-bonded silanols.

6. The IR Spectra of Py on H-ZSM5 (Figures 4 and 5): Hydrogen-Bonded Py, PyH^+, and PyH^+···Py Dimers

The adsorption of Py at RT (Figure 4a, curve 2, and Figure 4b, curve 1) causes the total disappearance of the

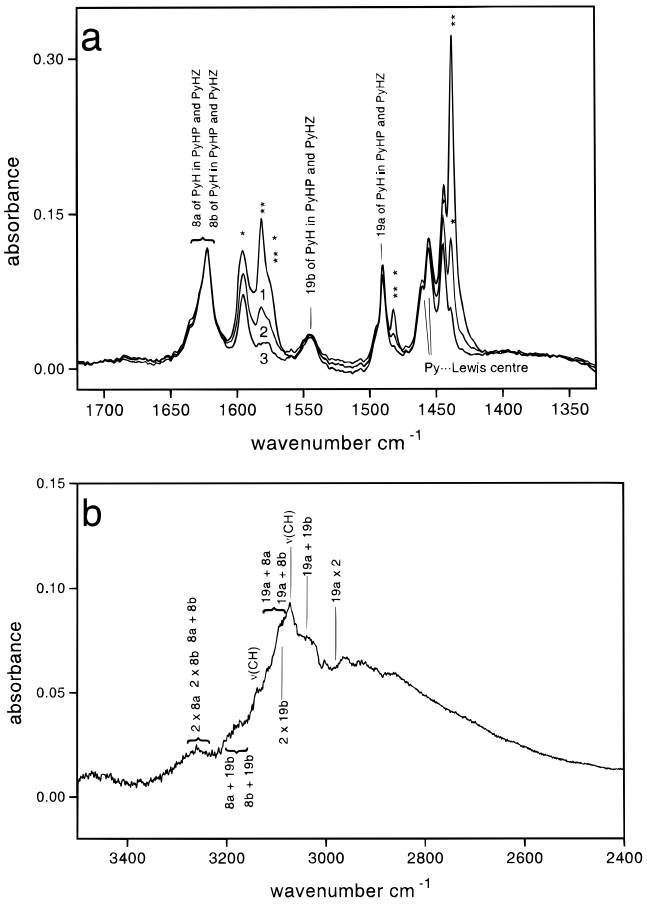

Figure 9. (a) Curves 1−3: details of the corresponding spectra of Figure 8a. One asterisk indicates (hb) Py; two asterisks indicate (ph) Py; PyH indicates pyridinium species; PyHP indicates pyridinium H-bonded with pyridine; and PyHZ indicates pyridinium H-bonded with the negatively charged zeolitic framework. (b) Details of spectrum 3 of Figure 8b. The overtone and the combination of the bands shown in Figure 9a are indicated with lines. The assignment is done without considering the selection rules.

ν(OH) bands of the silanols at 3745 cm^{-1} and of acidic groups at 3662 cm^{-1} (associated with AlOH groups involving partially extralattice Al) and at 3609 cm^{-1} (associated with framework AlOHSi Brönsted groups.)[14,25,32] This is the consequence of two type of reactions: (i) interaction with silanols following the path described in (1) with formation of hydrogen-bonded species. As the acid strength of the silanols is small, we expect that process 1 can be easily reversed simply by lowering the Py pressure (as already found for the silicalite−Py system); (ii) proton transfer from framework Brönsted sites to Py

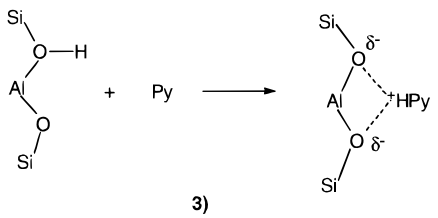

3)

and from partially extraframework Brönsted AlOH sites as well (scheme not shown for brevity) to give PyH^+ hydrogen bonded to the conjugated base $(SiOAlOSi)^-$ (hereafter Z^-). Process 3 is expected to be irreversible at RT.

(32) Misono, M. I.; Mizuno, Katamura, K.; Kasai, A.; Konishi, Y.; Sakata, K.; Okuhara, T.; Yoneda, Y. *Bull. Chem. Soc. Jpn.* **1982**, *55*, 400.

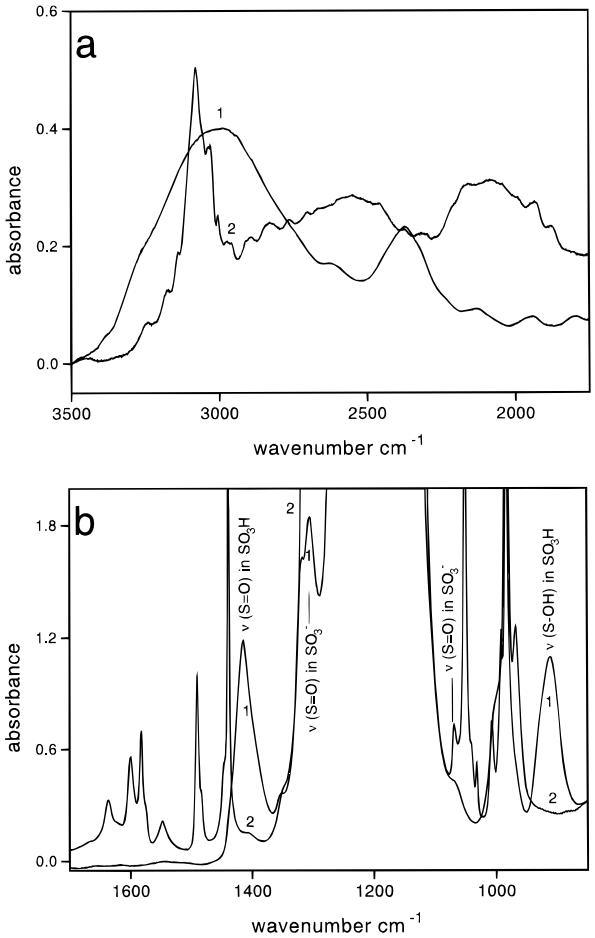

Figure 10. (a) Curve 1: H-Nafion background spectrum after outgassing under vacuum conditions at 383 K for 1 h. Curve 2: spectrum after equilibration with vapor pressure of Py in the spectral region 3500−1750 cm^{-1}. (b) As in part a except spectral region 1700−800 cm^{-1}.

As the HZ acid is strong, the conjugated bases (Z^-) should be rather weak and consequently the $Z^-\cdots{}^+HPy$ hydrogen bonding interactions are also expected to be weak. For this reason in the presence of excess Py a base displacement reaction is expected to partially occur up to the final equilibrium condition represented below:

$$Z^-\text{-----}PyH^+ + Py \rightleftharpoons PyH^+\text{-----}Py + Z^-$$

4)

The dimeric $PyH^+\cdots Py$ species are characterized by $NH^+\cdots N$ hydrogen bonds of at least comparable strength (or even greater strength than the $NH^+\cdots O^-$ species). For this reason it is expected that the equilibrium can be easily shifted to the left by simply lowering the Py pressure. Similar results have been obtained in heteropolyacids.[32]

On the basis of these expectations, it is evident that the broad absorption extending from 3250 to 1700 cm^{-1} (with an evident minimum at 2320 cm^{-1} evidenced by an arrow) appearing in Figure 4b and particularly prominent at the highest equilibrium pressures must be attributed to the stretching modes of $O^-\cdots HN^+$ and (more likely) of $NH^+\cdots N$ hydrogen-bonded groups in the species formed as shown in reactions 3 and 4. The minimum results from a Fermi resonance between the $\nu(NH^+\cdots N)$ (broad band extending in the 2800−1700 cm^{-1} interval with a maximum at ~2300 cm^{-1}) and the $2 \times \gamma(NH^+\cdots N)$. Due to the large anharmonicity of the involved modes, the resonance causes the formation of a characteristic Evans window.[5] The forma-

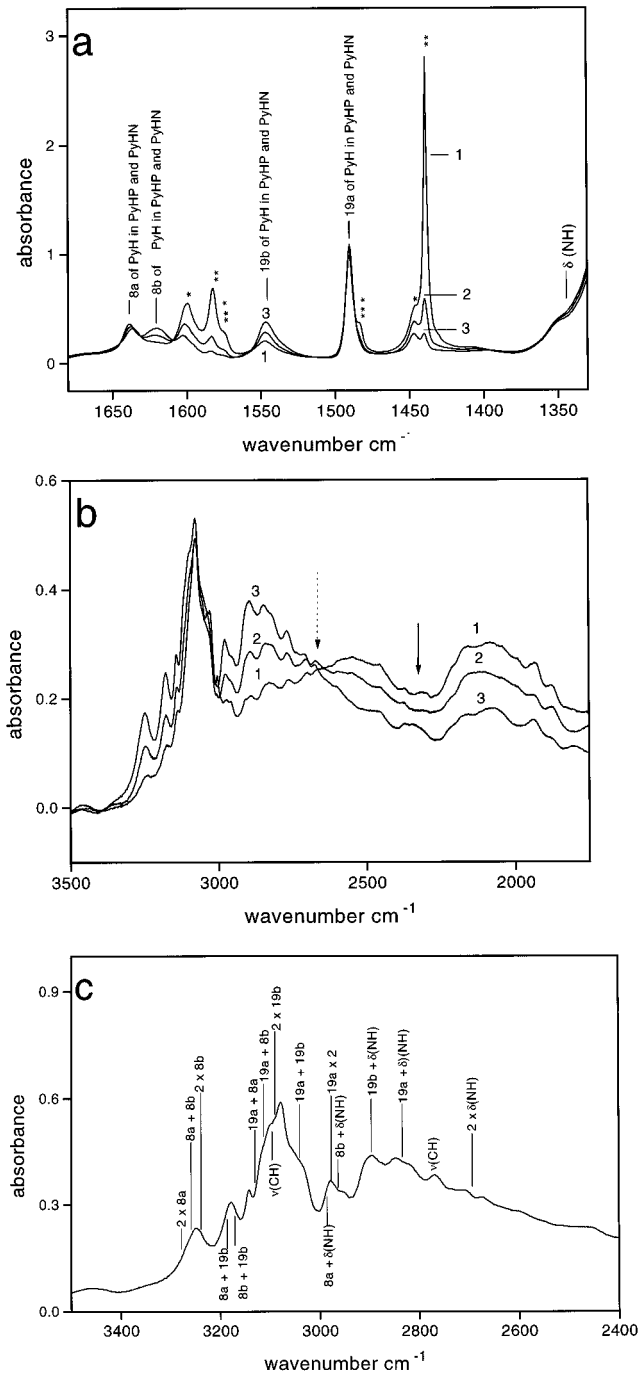

Figure 11. (a) Curve 1: spectrum of H-Nafion equilibrated with vapor pressure of Py. Curves 2 and 3: spectra, at increasing outgassing times at room temperature. One asterisk indicates (hb) Py; two asterisks indicate (ph) Py; PyH indicates pyridinium species; PyHP indicates pyridinium H-bonded with pyridine; and PyHN indicates pyridinium H-bonded with the SO_3^- groups. (b) Curve 1: spectrum of H−Nafion equilibrated with vapor pressure of Py. Curves 2 and 3: spectra at increasing outgassing times at room temperature. The arrow (full line) indicates an Evans window caused by a Fermi resonance of the ν(NH···) with the $2 \times \gamma$(NH$^+$···N) mode of the (PyH$^+$···P) dimer; the arrow (broken line) underlines the isosbestic point. (c) Spectrum 3 of Figure 11b. The overtones and combination bands of PyH$^+$···N (illustrated in Figure 11a) are indicated by lines. The assignment is done without considering the selection rules.

tion of a broad background upon adsorption of bases has been already reported and thoroughly discussed in ref 33.

For the reasons outlined before, the relative concentration of the various species formed in reactions 1, 3, and 4 are expected to change during the outgassing procedure at RT and this facilitates the distinction of the spectroscopic properties of the single species (*i.e.*, hydrogen-bonded Py, Z$^-$···HPy$^+$, and PyH$^+$···Py). In particular the various species are expected to disappear upon lowering the Py pressure in the following order: physically adsorbed species (ph) first, hydrogen-bonded species (hb) second, PyH$^+$···Py third, and finally PyH$^+$···Z$^-$ (which should be irreversible at RT). Inspection of Figures 4b and of 5a (where the difference spectra taken at increasing outgassing times at RT are reported) allows the following considerations to be derived: (i) the original silanol intensity is rapidly restored, as expected when Py hydrogen bonded to silanols located on external surfaces is removed; (ii) the ring modes of physically adsorbed and hydrogen-bonded Py (labeled with two and one asterisk, respectively) disappear in succession; (iii) the ν(CH) stretching modes of physically adsorbed and hydrogen-bonded Py also disappear (together with a broad underneath absorption in the 3200−2800 cm^{-1} range, *i.e.*, a frequency similar to that found on pure silicalite and due to the ν(OH···N) mode of hydrogen-bonded species).

From the previous observation and from the comparison with the spectra of Py adsorbed on silicalite and on silica,[30] we conclude that the variations observed in spectra 1−3 of Figure 5a are mainly due to desorption of Py physically adsorbed and Py hydrogen bonded to silanols following the reverse of reaction 1. The peaks at 1634−1638, 1623, 1547, 1491, and 1340 cm^{-1} are left nearly unperturbed by this evacuation procedure: consequently they mainly belong to internal modes of the PyH$^+$ moieties in PyH$^+$···Z$^-$ and PyH$^+$···Py complexes formed in reactions 3 and 4. Comparison of these frequencies with those of PyH$^+$ salts in various solvents (including the most basic ones) allows the assignment of the main bands: 1634−1638 cm^{-1} (8a ring mode), 1623 (8b), 1547 (19b), 1491 (19a), and 1340 cm^{-1} δ(NH) (modes symbols as in ref 34). The mode at 1547 cm^{-1} represents the most characteristic feature of the spectrum and is often used as a diagnostic probe of the formation of PyH$^+$. As it contains a considerable admixture of δ(NH), it can undergo a distinct broadening upon hydrogen-bonding perturbation: this explains its large half-width (at least when comparison is made with the 8a, 8b, and 19a modes which have similar frequency but have less δ(NH) character).

Evacuation leads to preferential transformation of the PyH$^+$···Py dimer into the PyH$^+$···Z$^-$ species (inverse of reaction 4). In fact we observe (i) a substantial decrement of the broad absorption extending in the 2800−1700 cm^{-1} range; (ii) a further decrement of the characteristic peaks of neutral Py (ph and hb); (iii) a modification of the 8a, 8b and 19b peaks of PyH$^+$ (the band at 1638 cm^{-1} distinctly shifts to 1634 cm^{-1} while the band at 1547 cm^{-1} becomes sharper). The behavior of the 1547 cm^{-1} peak (19b) is especially informative: in fact it becomes distinctly sharper upon evacuation (the intensity on the maximum apparently increases); this indicates that upon Py desorption, the PyH$^+$ becomes less perturbed by hydrogen bonding (as expected if the transformation of PyH$^+$···Py into PyH$^+$···Z$^-$ species is occurring); (iv) a spectacular modification of the 3300−2600 cm^{-1} range, where many bands are now clearly observable. These bands modulate the broad absorption covering the 3400−2200 cm^{-1} range (fwhm $\approx$ 700 cm^{-1}) which is the ν(NH) stretching of the PyH$^+$ hydrogen bonded to the zeolite skeleton Z$^-$. The

(33) Knözinger, H. In *The Hydrogen bond/III*: *Dynamics Thermodynamics and special systems*; Schuster, P., Zundel, G., Sandorfy, C., Eds.; North-Holland: Amsterdam, 1976; p 1261. Knözinger, H. *Surf. Sci.* **1974**, *41*, 339.

(34) Glazunov, V. P.; Odinokov, S. E. *Spectrochim. Acta* **1982**, *38A*, 399.

maximum of this absorption can be located at about 2750 cm^{-1}. As the frequency of the $\nu(NH^+)$ mode has been calculated to occur at $\nu = 3425\ cm^{-1}$ [35] it seems that the hydrogen-bonding interaction in $PyH^+\cdots Z^-$ complex causes a downward shift of $\Delta\nu \sim 700\ cm^{-1}$. These narrow bands are undoubtedly due to the Fermi resonances between the broad $\nu(NH\cdots Z^-)$ mode and the overtones and combinations of the PyH^+ ring stretching and bending (and of the δ and γ modes of the $NH^+\cdots Z^-$ group as well). This is demonstrated not only by the remarkable similarity of the observed frequencies with the calculated values (marked by lines in Figure 5b) but also by the comparison with the spectra of similar $PyH^+\cdots B^-$ compounds[34,36,37] (B^- represents an unspecific strong base). In conclusion the main spectroscopic features of the $Z^-\cdots PyH^+$ complexes can be summarized as follows:

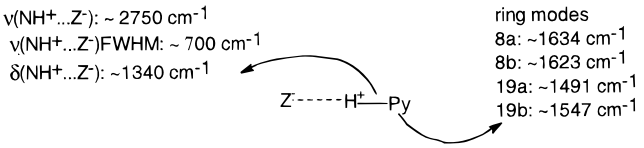

5)

It is most noticeable that the $\nu(NH^+\cdots N)$ mode of the dimer occurs at lower frequency and is definitely broader than the corresponding $\nu(NH^+\cdots Z^-)$ mode of the $PyH^+\cdots Z^-$ monomer: this is not unexpected since Z^- is probably a weaker base with respect to Py. This is equivalent to saying that $Z{-}H^+$ acid is stronger than PyH^+. Finally, a further question to answer is why are numerous and narrow-shaped Fermi resonances with the low-frequency modes of the PyH^+ moiety not observable in the spectrum of the $PyH^+\cdots Py$ dimer? We think that this is due to the broader character of some of the most frequently involved bands (for instance the 19b mode at 1547 cm^{-1}). In fact the stronger hydrogen-bonding perturbation present in the dimeric $PyH^+\cdots Py$ species broadens this fundamental mode (because it contains a considerable admixture of $\delta(NH)$) and so makes its overtone and the combination resonances too broad to be observable. In the end, only the strongest resonance associated with the $2 \times \gamma(NH^+\cdots N)$ overtone is appreciably altering the shape of the $\nu(NH^+\cdots N)$ band through the formation of a clear Evans window at 2300 cm^{-1}. It is most noticeable that similar spectra have been reported for the analogous dimers in solution.[34] At this point in the discussion it is probably appropriate also to answer a second question: why are Fermi resonance effects so spectacular in the $PyH^+\cdots Z^-$ spectra and not so prominent in the Py···HO-Si spectra (see for instance the Py- silicalite case), even if, in both cases, a substantial overlap exists between $\nu(NH^+\cdots Z^-)$ and $\nu(OH\cdots Py)$ with the overtones of the internal modes of PyH^+ and Py, respectively? The answer is straight forward and related directly to the arguments developed in the first answer: the strongest resonance effects are observed when the involved low frequency modes contain considerable admixture of modes (δ, γ) involving the hydrogen atoms of NH groups, *i.e.*, the atoms which are more directly participating in the hydrogen bonding.

7. The IR Spectra of Py on H-β (Figures 6 and 7)

There is strict similarity between the spectra of the Py/H-ZSM-5 and Py/H-β systems. This means that the same phenomena are occurring, *i.e.*: (i) pyridine protonation and subsequent formation of dimers; (ii) formation of hydrogen-bonded SiOH···Py; (iii) formation of physically adsorbed species. The IR spectra of $PyH^+\cdots Z^-$ and $PyH^+\cdots Py$ are essentially identical in the two cases, and no further comment is needed (the relevant assignments are indicated in Figures 6 and 7 and the corresponding captions). The great similarity between the spectra of $PyH^+\cdots Z^-$ in H-ZSM-5 and H-β indicates that the basic strength of Z^- for the two cases is nearly identical. This in turn implies that H-ZSM-5 and H-β also have very similar acidities. With respect to the Py/H-ZSM-5 system, the intensity of the peaks due to physically adsorbed Py (labeled with two asterisks in the figures) is remarkably large. This effect, observed only in H-β, is likely associated with the larger available volume which not only allows the formation of PyH^+ monomers and $PyH^+\cdots Py$ dimers but also leaves plenty of space for the formation of liquid-like (physically adsorbed) Py.

8. The IR Spectra of Py on H-Mordenite (Figures 8 and 9)

As already anticipated in section 4.4, Py adsorption on H-MORD is not accompanied by the total destruction of the Brönsted sites (only a small intensity decrease corresponding to consumption of ≈10% of the sites being observed, Figure 8a). As the acid strength of H-MORD is not substantially different from that of H-ZSM-5 and H-β, the only reasonable explanation is that the adsorption products initially formed on the external surface are blocking the channel entrances and so preventing the diffusion of Py toward more internal sites. In favor of this hypothesis we remark that, except for the definitely lower intensity and poor resolution, the bands are very similar to those found on H-ZSM-5 and H-β. This indicates that the involved species are necessarily the same (*i.e.*, $PyH^+\cdots Z^-$ and $PyH^+\cdots Py$, see the assignments schematically reported in Figures 8 and 9 and the corresponding captions). Our explanation of hindered diffusion is that the key factors are represented by the protonic concentration (much larger in H-MORD) and by the absence of interconnected channels, so preventing the bypass of an obstructed cavity. We believe that a layer of irreversibly adsorbed Py molecules is immediately formed at the channel mouth preventing any further diffusion through the bulk at RT.[38]

Previous studies on the interaction of N_2, CO, $CH_2{=}CH_2$, and $CH_3CH{=}CH_2$[15,16,29] with H-MORD indicate that diffusion limitations are not present for N_2 and CO reactants (because they originate only weakly bonded, reversible complexes) while they are observed for $CH_2{=}CH_2$ and $CH_3CH{=}CH_2$ whose quick oligomerization occludes the channels. Moreover the formation of extralattice Al (in the form of Al_2O_3 microparticles) can partially occlude the channel pores as well.[39] The interaction of Py with Lewis acid sites has already been deeply discussed in the literature, see *e.g.* refs 9, 13, 30, and 40−42; being that this argument is beside the purpose of the present contribution, we will not discuss it anymore.

(35) Kubelkovà, L.; Kotrla, J.; Florian, J. *J. Phys. Chem.* **1995**, *99*, 10285.
(36) Glazunov, V. P.; Odinokov, S. E. *Spectrochim. Acta* **1982**, *38A*, 409.
(37) Cook, D. *Can. J. Chem.* **1961**, *39*, 2009.
(38) Niessen, W.; Karge, H. G. In *Zeolites and Related Microporous Materials*: *State of the Art 1994*; Weitkamp, J., Karge, H. G., Pfeifer, H., Hölderich, W., Eds.; *Studies in Surface Science and Catalysis*; Elsevier: Amsterdam, 1994; Vol. 84B, p 1191.
(39) Miller, J. T.; Hopkins, P. D.; Meyers, B. L.; Ray, G. J.; Roginski, R. T.; Zajac, G. W.; Rosenbaum, N. H. *J. Catal.* **1992**, *138*, 115.
(40) Hughes, T. R.; White, H. M. *J. Phys. Chem.* **1967**, *71*, 2192.
(41) Morrow, A.; Cody, I. A. *J. Phys. Chem.* **1976**, *80*, 1995.
(42) Ashim, K.; Ghosh, K.; Curthoys, G. *J. Chem. Soc., Faraday Trans. 1* **1983**, *79*, 805.

9. The IR Spectra of $PyH^+\cdots SO_3^-$ and $PyH^+\cdots Py$ Formed on H-Nafion (Figures 10 and 11)

As already mentioned in the Introduction, the source of the superacidity in the Nafion membrane is represented by the SO_3H groups whose acid character is enhanced by the presence of fluorine in the polymer backbone. The main vibrational features of these groups can be clearly seen in the IR spectrum of the polymer outgassed at 383 K under vacuum (Figure 10a, curve 1) and can be summarized as follows: (i) ν(OH$\cdots$) is responsible for the broad and tailed band centered at 3000 cm^{-1} (fwhm $\cong$ 500 cm^{-1}). Unlike the ν(OH) of the closest monomeric analogue in the gas phase (CF_3SO_3H, triflic acid) observed at 3588 cm^{-1} (fwhm $\cong$ 20 cm^{-1}), the observed band is substantially shifted toward the lower frequency values and broadened. A nearly identical effect follows the formation of the hydrogen-bonded dimer in the gas phase.

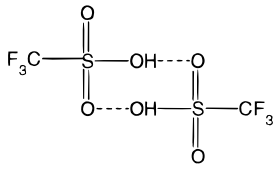

6)

Consequently it is inferred that the SO_3H groups in the dehydrated membrane are interacting similarly. The band at 2375 cm^{-1} (superimposed on the low-frequency tail of the main band) actually coincides with the overtone of a skeletal mode at 1180 cm^{-1}.[24] (ii) ν(S=O) is responsible for the band at 1413 cm^{-1}. This attribution is confirmed by its behavior upon interaction with proton acceptors (*vide infra*) and by its being absent in the spectrum of Na-Nafion (results not shown for brevity). (iii) ν(S−OH) is associated with the band at 910 cm^{-1} (fwhm $\cong$ 25 cm^{-1}). This band is slightly broadened by an indirect hydrogen-bonding effect. Also in this case the attribution is based on its disappearance upon interaction with proton acceptors (*vide infra*) and upon its absence in the spectrum of Na-Nafion.[24]

The remaining bands appearing in Figure 10b (bands at 1250−1100 and 980 cm^{-1}) are mainly associated with modes of the skeleton: this is demonstrated by their unaltered presence on deprotonated and on Na-exchanged Nafion. Finally the smaller bands at 1315−1300 (doublet) and at 1060 cm^{-1} must be attributed to the stretching modes of SO_3^- species, present in low concentration, possibly formed by self-protonation.[24] Unlike zeolites H-Nafion is unique in that it allows the direct observation of the spectroscopic properties of many internal modes of the proton donor groups (and of their modifications upon interaction with the adsorbates). For this reason it is an excellent training ground for the study of all the reactions where the proton is involved. When the interaction with Py is considered,

7)

the extent of protonation can be monitored not only by the appearance of the modes of PyH^+ and the destruction of the ν(OH$\cdots$) mode of the Brönsted group (like on H-ZSM-5, Hβ, and H-MORD) but also by the destruction of the internal modes of the SO_3H group and the simultaneous appearance of the modes of the SO_3^- species. This new characteristic can be of vital importance in all cases where the spectra of the internal modes of protonated ($^+$HB) and unprotonated bases B cannot be distinguished and when the spectra in the high-frequency region cannot be unambiguously assigned to one of the two structures:

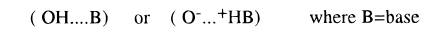

8)

As can be clearly seen from Figure 10b when the system is equilibrated with Py at the saturation pressure, all the manifestations of the SO_3H groups disappear, while those characteristic of PyH^+ (peaks at 1638, 1619, 1546, and 1489 cm^{-1} fully assigned in Figure 11a), of δ(NH) at ~1350 cm^{-1} and of SO_3^- (peaks at 1315−1300 and 1060 cm^{-1}) simultaneously grow up (reaction 7). At this pressure the bands of neutral Py (seen in Figure 11a, the bands with an asterisk) are also clearly visible.

When the 3500−1750 cm^{-1} region is explored (Figure 11b), we notice (i) the presence of an extremely broad absorption extending in the 3350−1750 cm^{-1} range with a minimum at 2350 cm^{-1} evidenced by an arrow in Figure 11b; (ii) a complex envelope of narrower bands in the 3250−2650 cm^{-1} range.

Comparison with the spectra of Py adsorbed on H-ZSM-5, H-β, and H-MORD (under comparable pressure conditions) allows us to immediately assign the two broad bands at 2500 and 2100 cm^{-1} to the spectroscopic manifestations of ν($NH^+\cdots$N) in the $PyH^+\cdots$Py complexes (in practice, the two bands are generated by an Evans window at 2350 cm^{-1} due to a Fermi resonance with a 2 × γ($NH^+\cdots$N) overtone. The envelope of narrower bands in the 3250−2650 cm^{-1} interval is partially due to the ν(CH) modes of both Py and PyH^+ in $PyH^+\cdots$Py complexes (bands in the 3100−3000 cm^{-1} interval) and partially to the contribution of Fermi resonance effects between the broad ν($NH^+\cdots$N) and the overtones and the combination of PyH^+ ring modes. In conclusion, in the presence of excess Py the following equilibrium is established:

9)

By analogy with the Py/H-ZSM-5 system, it is expected that outgassing at RT can remove the weakly adsorbed Py (with a subsequent shift of the equilibrium to the left and formation of $SO_3^-\cdots{}^+$HPy species). In fact we notice (i) the gradual disappearance of the bands of neutral Py either physically adsorbed or interacting with PyH^+ through hydrogen bond); (ii) the familiar, characteristic, and spectacular Fermi resonance modulation of the ν($NH^+\cdots$) mode, centered at about 2950 cm^{-1}, in the $SO_3^-\cdots{}^+$HPy complexes (for a complete classification of the bands, see Figure 11c) already encountered in the spectra of $PyH^+\cdots Z^-$ complexes; (iii) the characteristic narrowing of the band at 1547 cm^{-1} (19b mode) and the small modification of modes 8a and 8b associated with the shift to the left of equilibrium 9; this effect was also encountered before. Notice how only the bands belonging to modes 8a, 8b, and 19b containing an admixture of δ(NH$\cdots$) vibration are showing this behavior; (iv) the outgassing procedure is not altering the intensity of the bands of the SO_3^- species, as expected.

The equilibrium between PyH^+ monomer and $PyH^+\cdots$Py dimer is evidenced by the presence of an isosbestic point at 2800 cm^{-1} (see the arrow (broken line) in Figure 11b). It is most interesting that the maximum of the ν(NH) band in $PyH^+\cdots$Nafion$^-$ complexes is observed at about 2950 cm^{-1}, *i.e., at a freqency higher than that observed for the PyH$\cdots Z^-$ adducts*. This different shift is associated with the smaller basicity of Nafion$^-$ with respect

to Z^-. This observation in turn implies that H-Nafion is an acid stronger than H-ZSM-5, H-β, and H-MORD.

10. Conclusions

The interaction of Py with different acidic zeolites and with the superacid polymer Nafion has been studied by infrared spectroscopy in a carefully controlled environment. In all cases Py reacts quantitatively with the available acid sites to form pyridinium species. These species interact by hydrogen bonding either with the negatively charged zeolite framework (or fluorinated backbone), at low Py concentrations, or with other Py molecules to form a dimer, at higher concentrations. While forming the same chemical species, the different solids differ in the amount of acid sites accessible to the adsorbed molecules. In zeolites H-ZSM-5 and H-β, possessing a three-dimensional system of interconnected channels and a low acid site concentration, all acid sites react readily. At high loads, an increased amount of Py adsorbed reversibly, consisting of molecules physisorbed in the internal channels and hydrogen bonded to silanol groups on the external surfaces and at internal defects. The unidirectional channels of zeolite mordenite, on the contrary, are easily occluded by the first irreversibly adsorbed molecules, thus stopping further diffusion in the bulk. This is also favored by the higher concentration of acid sites. Moreover, the side pockets of the main channels and the acid sites therein are not accessible to Py due to their too small size. On the H-Nafion polymer, slow diffusion is also observed, but all acid sites can be consumed with long contact times. The adsorption and reaction of Py involves the swelling of the dense polymer and the breaking of the SO_3H-SO_3H hydrogen bonds present in the evacuated sample. The hydrogen bond of pyridinium ion to pyridine is stronger than that to the conjugated zeolite base, as demonstrated by the lower $\nu(NH^+\cdots N)$, but the equilibrium between the two forms can be shifted easily by varying the Py load. In all the observed hydrogen-bonded systems the broad $\nu(NH^+\cdots N)$ absorption is modulated by resonances with overtones and combination modes of the 8a, 8b, 19a, and 19b ring stretching and $\delta(NH\cdots)$ modes of pyridinium. Moreover, Fermi resonance with the $2 \times \gamma(NH)$ of $(PyH^+\cdots Py)$ causes the appearance of a pronounced Evans window at 2300 cm^{-1} in the spectrum of the dimer.

Acknowledgment. This work has been supported by MURST and CNR (Progetto strategico Tecnologie Chimiche Innovative).

LA950571I